



The Timing of Neural Stem Cell-Based Virotherapy Is Critical for Optimal Therapeutic Efficacy When Applied With Radiation and Chemotherapy for the Treatment of Glioblastoma

ALEX L. TOBIAS,^a BART THACI,^a BRENDA AUFFINGER,^a ESTHER RINCÓN,^a IRINA V. BALYASNIKOVA,^a CHUNG KWON KIM,^a YU HAN,^a LINGJIAO ZHANG,^a KAREN S. ABOODY,^b ATIQUE U. AHMED,^a MACIEJ S. LESNIAK^a

Key Words. Glioma • Gene therapy • Neural stem cell • Adenovirus • Virotherapy • Radiation • Chemotherapy • Temozolomide

ABSTRACT

Glioblastoma multiforme (GBM) remains fatal despite intensive surgical, radiotherapeutic, and chemotherapeutic interventions. Neural stem cells (NSCs) have been used as cellular vehicles for the transportation of oncolytic virus (OV) to therapeutically resistant and infiltrative tumor burdens throughout the brain. The HB1.F3-CD human NSC line has demonstrated efficacy as a cell carrier for the delivery of a glioma tropic OV CRAd-Survivin-pk7 (CRAd-S-pk7) in vitro and in animal models of glioma. At this juncture, no study has investigated the effectiveness of OV-loaded NSCs when applied in conjunction with the standard of care for GBM treatment, and therefore this study was designed to fill this void. Here, we show that CRAd-S-pk7-loaded HB1.F3-CD cells retain their tumor-tropic properties and capacity to function as in situ viral manufacturers in the presence of ionizing radiation (XRT) and temozolomide (TMZ). Furthermore, for the first time, we establish a logical experimental model that aims to recapitulate the complex clinical scenario for the treatment of GBM and tests the compatibility of NSCs loaded with OV. We report that applying OV-loaded NSCs together with XRT and TMZ can increase the median survival of glioma bearing mice by approximately 46%. Most importantly, the timing and order of therapeutic implementation impact therapeutic outcome. When OV-loaded NSCs are delivered prior to rather than after XRT and TMZ treatment, the median survival of mice bearing patient-derived GBM43 glioma xenografts is extended by 30%. Together, data from this report support the testing of CRAd-S-pk7-loaded HB1.F3-CD cells in the clinical setting and argue in favor of a multimodality approach for the treatment of patients with GBM. STEM CELLS TRANSLATIONAL MEDICINE 2013;2:000–000

INTRODUCTION

Glioblastoma multiforme (GBM) is the most common and fatal of all primary brain tumors and is considered largely incurable [1, 2]. The prognosis for GBM patients remains uniformly poor because of the infiltrative nature and high rate of recurrence [3]. Despite the aggressive standard of care consisting of surgical resection, radiation (XRT), and temozolomide (TMZ)-based chemotherapy, median survival is still 14.6 months [4], with only 26% of patients alive at 2 years [5]. Although current therapy options provide a modest increase in survival, many factors, including GBM's intrinsic ability to effortlessly permeate surrounding brain tissue and acquire resistance to conventional therapies, limit current therapeutic efficacy [6–8]. Because of these barriers, there is an overwhelming need for the development of novel therapies.

In the last decade, stem cells have been evaluated as therapeutic agents in a wide variety of central nervous system diseases, including gliomas [9, 10]. The human neural stem cell (NSC) line HB1.F3-CD has been approved by the Food and Drug Administration for use in clinical trials, and our laboratory has used it as a cell carrier to achieve targeted delivery of CRAd-Survivin-pk7 (CRAd-S-pk7), a conditionally replicating adenovirus that confers glioma selectivity through the tumor-specific survivin promoter and fiber modification, to GBM [11–16]. We have shown that HB1.F3-CD cells act as in situ virus factories by supporting replication and release of antitumoral viral progeny while also protecting the therapeutic viral load from the host antiviral immune response [13]. Furthermore, intratumoral delivery of NSCs loaded with CRAd-S-pk7 impedes tumor growth and increases median survival by ~50% in an orthotopic xenograft model

^aBrain Tumor Center, University of Chicago, Chicago, Illinois, USA;

^bDepartment of Neuroscience, City of Hope National Medical Center and Beckman Research Institute, Duarte, California, USA

Correspondence: Maciej S. Lesniak, M.D., Brain Tumor Center, University of Chicago, 5841 South Maryland Avenue, MC 3026, Chicago, Illinois 60637, USA. Telephone: 773-834-4757; Fax: 773-834-2608; E-Mail: mlesniak@surgery.bsd.uchicago.edu

Received March 2, 2013; accepted for publication May 14, 2013; first published online in SCTM EXPRESS August 7, 2013.

©AlphaMed Press
1066-5099/2013/\$20.00/0

<http://dx.doi.org/10.5966/sctm.2013-0039>

of human glioma when compared with animals treated with CRAd-S-pk7 virus alone [13]. Importantly, CRAd-S-pk7-loaded HB1.F3-CD cells injected intracranially in nude mice bearing human glioma xenografts retain their tumor-tropic properties, replicate and release viral progeny for more than a week after reaching the tumor site, and hand off CRAd-S-pk7 to glioma cells *in vivo*. These data support both the efficacy and safety of this cell carrier-based anti-glioma oncolytic virotherapy.

In order to advance our NSC-based virotherapy toward a clinical trial, it is prudent to characterize the safety profile and efficacy of the novel therapy in an adjuvant setting with the current standard of care for GBM, radio- and chemotherapy (XRT-TMZ). There have been several reports that suggest virus-based gene therapies may be compatible and beneficial to use in combination with standard surgery, radiation, and chemotherapy. In pre-clinical models, the oncolytic virus (OV) G47 Δ acts synergistically with TMZ in effectively killing glioma stem cells, an important population of glioma cells believed to be significant for disease initiation, advancement, recurrence, and resistance to conventional therapy [17]. In the clinical setting, oncolytic reovirus given to patients in combination with chemotherapy was well tolerated in a phase I/II clinical trial for treatment of head and neck cancers [18]. Furthermore, in a phase II/III clinical trial that enrolled 36 patients with glioma, patients who received the experimental arm consisting of adenovirus encoding HSV-Tk and intravenous ganciclovir injections followed by postoperative radiotherapy survived 24.7 weeks longer than patients who received standard postoperative radiotherapy alone [19].

Therefore, because of the promising interactions between viruses and conventional therapy, it becomes prudent to investigate the three-way cooperation between cell carrier, oncolytic adenovirus, and conventional XRT-TMZ for the treatment of glioma. To date, no one has previously investigated the interactions of these three therapies, and a detailed understanding is crucial before this novel approach can be evaluated in a phase I clinical trial. Therefore, for the first time, we report on the therapeutic efficacy and safety monitoring of CRAd-S-pk7-loaded NSCs in the presence of XRT-TMZ for the treatment of human GBM. The goals of this study were to mimic the clinical situation in an experimental model and develop a clinically relevant protocol for combining stem cell-based oncolytic therapy with conventional treatment for GBM patients. Here we demonstrate that combining stem cell-based oncolytic therapy with XRT-TMZ does not negatively impact the properties of stem cells as a virus carrier or manufacturer *in situ*. Furthermore, in an orthotropic xenograft model of human glioma established with a patient-derived GBM line, CRAd-S-pk7-loaded NSCs administered intracerebrally in concurrence with XRT-TMZ treatment extended the median survival of mice when compared to treatment with XRT-TMZ alone. Moreover, NSCs should be administered prior to XRT-TMZ treatment because of the possible radiosensitizing effect of oncolytic adenovirus to glioma cells. Thus, data presented in this study will allow us to evaluate an NSC-based cell carrier for the targeted delivery of anti-glioma oncolytic virotherapy and develop a rational clinical protocol for the filing of a future investigational new drug (IND) application for a human clinical trial involving recurrent and newly diagnosed patients with malignant glioma.

MATERIALS AND METHODS

Cell Culture

HB1.F3-CD, a *v-myc* immortalized human NSC line, originated from the human fetal brain and was modified to constitutively express cytosine deaminase (CD) [20, 21]. Glioma cell lines U87MG and U251MG were purchased from the American Type Culture Collection (Manassas, VA, <http://www.atcc.org>), whereas GBM43-Fluc and GBM39, both primary human glioma specimens isolated from patients, were kindly provided by Dr. C. David James of the University of California, San Francisco. All adherent cultures were maintained in Dulbecco's modified Eagle's medium (Cellgro, Manassas, VA, <http://www.cellgro.org>) supplemented with 10% fetal bovine serum (Atlanta Biologicals, Lawrenceville, GA, <http://www.atlantabio.com>), 2 mmol liter⁻¹ L-glutamine, 100 units ml⁻¹ penicillin, 100 μ g ml⁻¹ streptomycin, and 0.25 μ g ml⁻¹ amphotericin B (Invitrogen, Carlsbad, CA, <http://www.invitrogen.com>). For more details regarding subculture and *in vivo* passaging, please refer to supplemental online data.

Viral Vectors

The replication-competent adenoviral vector CRAd-S-pk7 is made up of two genetic mutations to confer tumor selectivity and replication: (a) a fiber modification by the insertion of seven polylysine (pk7) into the C terminus of the wild-type fiber protein and (b) a survivin promoter inclusion upstream of the viral E1A gene [11]. CRAd-S-pk7 was used for viral loading of NSCs at 50 infectious units (IU) per cell for 1.5 hours at \sim 23°C in a suspension of 1×10^6 cells per 100 μ l of phosphate-buffered saline (PBS) or as adherent cells for all experiments [12–14]. ONYX-015 adenovirus was used only in immunoblotting experiments at the infectious dose of 50 IU per cell.

Chemotherapy and Radiotherapy

For all studies, the cells and mice received XRT in accordance with the University of Chicago's radiation safety guidelines and protocols. All cells received a single dose of 2 Gy XRT. For animal studies, 10 Gy fractionated dose radiotherapy (2 Gy for 5 consecutive days) was used. The animals were irradiated with a lead cover shielding their entire body, with only their heads exposed. For *in vitro* studies, cells were administered TMZ based on their IC₅₀ values when also treated with XRT simultaneously, which were as follows: HB1.F3-CD = 15 μ M; U251 = 44 μ M; U87 = 25 μ M; GBM43 = 37 μ M; and GBM39 = 50 μ M. For *in vivo* studies, the mice received 2.5, 5, 10, or 30 mg/kg TMZ via intraperitoneal injection. TMZ preparation and dilution are described in the supplemental online data.

Flow Cytometry

For detection of surface antigens, the cells were stained with primary antibodies for 1 hour at 4°C in fluorescence-activated cell sorting (FACS) buffer (0.5% bovine serum albumin + 0.05% sodium azide) in PBS. After the cells were washed, secondary antibodies were added in FACS buffer for 0.5 hour at 4°C. After fluorescent labeling, the samples were washed and acquired on a BD FACSCanto cytometer (BD Biosciences, Franklin Lakes, NJ, <http://www.bdbiosciences.com>) and analyzed using FlowJo (Tree Star, Ashland, OR, <http://www.treestar.com>). The following primary antibodies were used: fluorescein isothiocyanate (FITC)-conjugated anti-Oct4 (Millipore, Billerica, MA, <http://www.millipore.com>).

www.millipore.com), phosphatidylethanolamine (PE)-conjugated anti-Nestin (BD Biosciences), biotinylated Sox2 (R&D Systems, Minneapolis, MN, <http://www.rndsystems.com>), and PE-conjugated active caspase-3 (BD Biosciences). For a secondary antibody, streptavidin conjugated to Alexa 647 (Invitrogen) was used. All antibody dilutions were used according to the manufacturer's recommendation.

Evaluation of Relative Gene Expression by Quantitative Real-Time Polymerase Chain Reaction

Relative expression of mRNA transcripts was evaluated for the human receptors vascular endothelial growth factor receptor 2 (VEGFR2), CXCR4, CD44, and urokinase plasminogen activator receptor (uPAR) after exposure to 2 Gy of XRT and 15 μ M TMZ for 12 and 24 hours. Transcript levels were measured and analyzed using quantitative real-time polymerase chain reaction (qRT-PCR) as explained in the supplemental online data.

Assessment of NSC Migration

To analyze the migratory capacity of loaded HB1.F3-CD cells to tumor cells in the presence of XRT-TMZ treatment, a wound healing assay was carried out using cell culture inserts (catalog no. 80209; Ibbidi, München, Germany, <http://www.ibidi.de>). The specific protocol is defined in the supplemental online data. Migration analysis was conducted by measuring the average distance traveled as compared with that of mock cells.

Analysis of Viral Replication

To detect the level of viral replication, NSCs were infected with 50 IU of CRAAd-S-pk7 and treated with XRT-TMZ. Cells were collected, and the total DNA was isolated from cultured cells using a DNeasy tissue kit (Qiagen, Valencia, CA, <http://www.qiagen.com>). Adenoviral E1A gene expression was quantified via qRT-PCR using iQ SYBR Green supermix (Bio-Rad, Hercules, CA, <http://www.bio-rad.com>), using primers and protocol described elsewhere [22]. The analysis of samples is described in the supplemental online data. The quantification of infectious viral progeny of NSCs was conducted using the Adeno-X rapid titer kit protocol (Clontech, Mountain View, CA, <http://www.clontech.com>) as described elsewhere [12]. The titration unit (IU/ml) values quantified through this protocol are similar to plaque-forming units.

In Vitro Glioma Cell Toxicity Studies

A green fluorescent protein (GFP) expressing HB1.F3-CD cell line was generated as described elsewhere [13]. GBM43-Fluc cells were plated in 12-well plates and cocultured with HB1.F3-CD-GFP cells loaded with CRAAd-S-pk7 in the following NSC to glioma cell ratios: 1:0, 1:2, 1:5, 1:10, and 1:50. After 96 hours, the cells were collected, lysed with reporter lysis buffer (Promega, Madison, WI, <http://www.promega.com>), and added to luciferase assay reagent (Promega) according to the manufacturer's protocol. Following lysate preparation, the mean fluorescence intensity (MFI) was estimated for each group of cocultured cells using the GloMax 20/20 Luminometer (Promega). The mean luciferase intensity values were represented as the percentage of cells viable compared with mock cells.

U251, U87, and GBM39 cell viability was determined using 3-(4,5-dimethylthiazol-2-yl)-2,5-diphenyltetrazolium bromide (MTT) cell proliferation kit (Roche Diagnostics, Mannheim, Germany, <http://www.roche-applied-science.com>). The viability was subse-

quently determined by MTT as described by the manufacturer's protocol. Cell viability was expressed as the percentage of cells alive compared with the dimethyl sulfoxide-treated control.

Animal Experiments

All of the animals were cared for according to a study-specific animal protocol certified by the University of Chicago Institutional Animal Care and Use Committee. The animals underwent intracranial stereotactic surgery, and 3.5×10^5 GBM43 cells were implanted in a 2.5- μ l volume of PBS. For a detailed animal surgery and treatment protocol, please refer to the supplemental online data. For measurement of tumor volume on day 5, the mice were imaged for Fluc activity following intraperitoneal injection of D-luciferin (Gold Biotechnology, St. Louis, MO, <http://www.goldbio.com>) (4.5 mg per animal in 150 μ l of saline), and photon counts were recorded 10 minutes after D-luciferin administration by using a cryogenically cooled high-efficiency charged-coupled device camera system (Xenogen IVIS200 optical imaging system; Caliper Life Sciences, Mountain View, CA, <http://www.caliper.com>) [13]. Representative hematoxylin- and eosin-stained mouse brain tissue pictures were captured with an AxioCam Color MR digital camera attached to an Olympus BX41 microscope and rendered in AxioVision version 3.0 software.

Western Blot

For protein analysis, U87 or U251 cells were cultured in 100-mm plates. The cells were harvested, washed, and lysed by the addition of 200 μ l of mammalian protein extraction reagent (Pierce, Rockford, IL, <http://www.piercenet.com>) supplemented with protease and phosphatase inhibitor cocktail. 40 μ g of protein per lane was run on 10% Tris-HCl gel and was transferred by semidry electrophoretic transfer onto a polyvinylidene difluoride membrane. The membrane was blocked with 2% nonfat dry milk and stained with anti-Mre11 (Cell Signaling Technology, Danvers, MA, <http://www.cellsignal.com>), anti-Rad50 (Cell Signaling Technology), and anti- β -actin (Santa Cruz Biotechnology, Dallas, TX, <http://www.scbt.com>) antibodies, followed by the secondary anti-rabbit antibody conjugated with HRP (Cell Signaling Technology). All antibodies were diluted according to the manufacturer's recommendation. ImmunStar WesternC was used to develop the reaction. Images were captured using Bio-Rad's ChemiDoc imaging system.

Immunofluorescence

GBM43 cells were grown directly in four-well chamber slide (Lab-Tek, Hatfield, PA, <http://www.labtek.net>) cell culture dishes. The cells were fixed and stained according to the manufacturer's protocol. The anti-phosphohistone H2A.X (Cell Signaling Technology) primary antibody was used at a 1:600 dilution overnight at 4°C. For immunofluorescence of animal tissue, the brains were embedded in optimal cutting temperature compound (Tissue-Tek) and frozen in a dry ice-2-methylbutane bath. Sections of 8 μ m, spanning \sim 2 mm of tissue, were stained according to the manufacturer's protocol. The anti-cleaved caspase-3 (Cell Signaling Technology) primary antibody was used at a 1:600 dilution overnight at 4°C. The cells and tissues were washed, and goat anti-rabbit antibody conjugated with FITC (Santa Cruz Biotechnology) secondary antibody was added for 2 hours at \sim 23°C in the dark. Secondary antibody was diluted according to the manufacturer's recommendation. After incubation with secondary

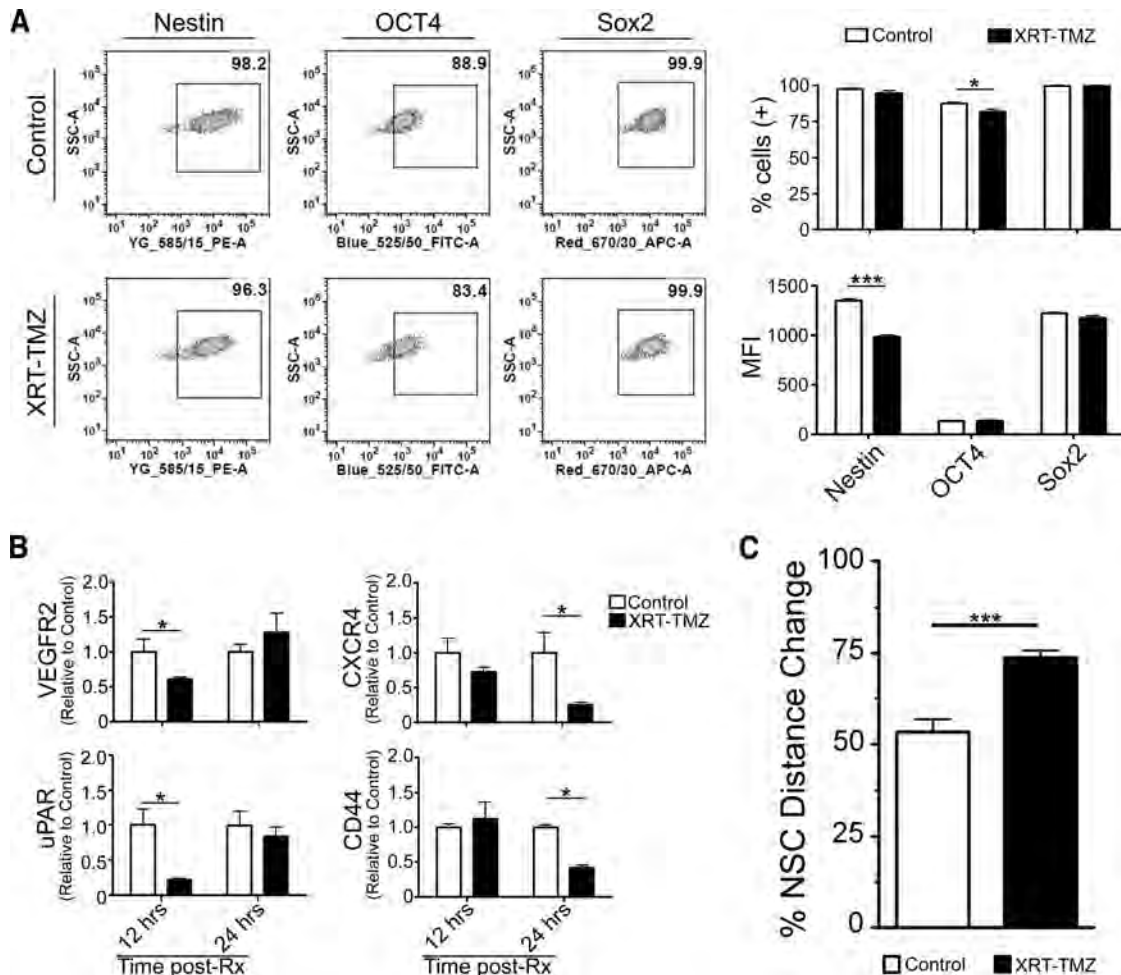


Figure 1. Characterization of surface markers and migration of loaded NSCs treated with XRT-TMZ. **(A):** Surface marker expression of irradiated and chemotherapy-treated NSCs at 24 hours as analyzed by fluorescence-activated cell sorting (FACS). Shown are representative FACS plots (left) and the percentage of positive and mean fluorescent intensity of the surface markers of untreated compared with treated neural stem cells (right). **(B):** Transcription level of surface receptors associated with NSC migration at 12 and 24 hours after XRT-TMZ treatment. Relative mRNA transcripts were analyzed by quantitative real-time polymerase chain reaction and were compared with untreated NSCs. **(C):** Functional migration of XRT-TMZ-treated NSCs at 48 hours after treatment. The percentage of distance change was greater for XRT-TMZ-treated NSCs than untreated control NSCs. *, $p < .05$; ***, $p < .001$. Abbreviations: APC, allophycocyanin; FITC, fluorescein isothiocyanate; MFI, mean fluorescence intensity; NSC, neural stem cell; PE, phosphatidylethanolamine; Rx, radiation therapy-temozolomide therapy; SSC, side scatter; TMZ, temozolomide; uPAR, urokinase plasminogen activator receptor; VEGFR, vascular endothelial growth factor receptor; XRT, radiation therapy.

antibody, the cells and tissues were washed and mounted with ProLong Gold antifade reagent with 4',6-diamidino-2-phenylindole (Molecular Probes). All images were captured on a Zeiss Axiovert 200M inverted fluorescent microscope.

Statistical Analysis

All of the statistical analyses were performed using GraphPad Prism 4 (GraphPad Software Inc., San Diego, CA, <http://www.graphpad.com>). The data represent the results for assays performed in triplicate or more, and all values were calculated as means \pm SE. For continuous variables, comparisons between groups were made using Student's *t* test or analysis of variance with Bonferroni or Dunnett's post hoc test. Survival curves were generated by the Kaplan-Meier method, and the log-rank test was used to compare the distribution of survival times. All reported *p* values were two-sided and were considered statistically significant at a *p* value of $< .05$ (***, $p < .001$; **, $p < .01$; *, $p < .05$).

RESULTS

Neural Stem Cells Retain Their Migratory Properties in the Presence of Irradiation and Temozolomide

NSCs have an inherent pathotropism toward glioma, which is critical for their utility as cell carriers. Therefore, it is critical that such intrinsic molecular properties and phenotypes of NSCs are maintained during radio-chemotherapy (XRT-TMZ). Thus, we first evaluated whether general stem cell characteristics would be altered during therapy. Pharmacokinetic studies have revealed that the peak concentration of TMZ measured in a patient's blood is $50 \mu\text{mol/l}$ [23–26] and $5 \mu\text{mol/l}$ in the cerebral spinal fluid [26], and we speculate that the intratumoral concentration of TMZ may be in the range of 5–50 μM . Therefore, we set out to evaluate NSC properties after exposure to 15 μM TMZ, the IC_{50} for HB1.F3-CD cells in vitro (data not shown), in combination with 2 Gy of ionizing radiation [27]. As shown in Figure 1A, at 24 hours after exposure to conventional therapy, the NSC

markers Nestin and Sox2 were found present in almost all the adenovirus-loaded control cells ($97.4 \pm 0.8\%$ and $99.8 \pm 0.2\%$, respectively). Oct4, a marker of self-renewal for undifferentiated cells, was expressed in $87.6 \pm 1.1\%$ of the loaded NSCs. We observed that Sox2 expression levels were not significantly altered from XRT-TMZ therapy; however, Nestin and Oct4 decreased slightly. The percentage of Oct4 positive cells decreased to $81 \pm 2\%$ (*, $p < .05$), whereas the MFI was not reduced. For Nestin, we observed the reverse: the percentage of positive cells remained unchanged, whereas the MFI was reduced by 27% (***, $p < .001$) (Fig. 1A). Because of the high priority of safety when working with the undifferentiated *v-myc* immortalized HB1.F3-CD stem cell line [20], we performed an in vivo safety monitoring experiment to test the effect of XRT-TMZ on loaded HB1.F3-CD cellular transformation. CRAd-S-pk7-loaded NSCs were implanted in the brains of nude mice with no tumor burden. Subsequently, 1 day after implantation mice received 30 mg/kg of TMZ and 2 Gy of radiation for 5 consecutive days. The mice were monitored for weight loss and survival, and at the end of >4 months, the mice that were injected with loaded NSCs and treated with XRT-TMZ showed no significant weight loss or other symptoms of malignant transformation (supplemental online Fig. 1).

Furthermore, the capacity of NSCs to home to glioma cells has been linked to the expression of chemoattractant receptors expressed on their surface [28]. Therefore, we next evaluated the transcription level of various chemokine receptors that have been attributed to the migration of NSCs both in the absence and presence of XRT-TMZ at 12 and 24 hours after treatment. We noticed that VEGFR2 and uPAR transcription was inhibited transiently at 12 hours (*, $p < .05$) and recovered at 24 hours in the presence of XRT-TMZ. Moreover, CD44 and CXCR4 expression was found reduced only after 24 hours of treatment, *, $p < .05$ (Fig. 1B). To evaluate whether these fluctuations in transcription of chemokine receptors had any effect on the functional pathotropism of loaded carrier cells, we performed a wound healing assay. We found that XRT-TMZ did not reduce but rather increased the migration of loaded NSCs in vitro (***, $p < .001$) (Fig. 1C). Taken together, we conclude that the exposure to conventional anti-glioma therapies exerts a minimal effect on the phenotypic and chemoattractant markers of NSCs but does not alter their tumor-tropic migration.

Radio-Chemotherapy Minimally Reduces Oncolytic Virus Replication Within Carrier Cells

In order for a stem cell to be an effective carrier of OV, it must support viral replication. To determine the impact of XRT-TMZ treatment on the ability of NSCs to replicate CRAd-S-pk7, viral replication was quantified by viral E1A DNA copy number or infectious progeny present in NSCs. As shown in Fig. 2A, TMZ had a bimodal effect on the adenoviral E1A gene copies (E1A per nanogram of DNA). On days 1 and 2, we noticed that TMZ at 100 and 50 μM , respectively, increased the E1A copies per nanogram of DNA between 2.5- and 4.5-fold (*, $p < .05$). No difference was noted on day 3, whereas there was a 3-fold decrease in E1A copies per nanogram of DNA on day 4 at the highest TMZ concentration of 100 μM (*, $p < .05$).

Similar to TMZ, 2 Gy irradiation showed a trend toward increased E1A copy number on day 1, followed by a significant reduction of E1A copy on day 3 (*, $p < .05$) (Fig. 2B). In order to quantify the effect of concurrent XRT-TMZ on viral replication,

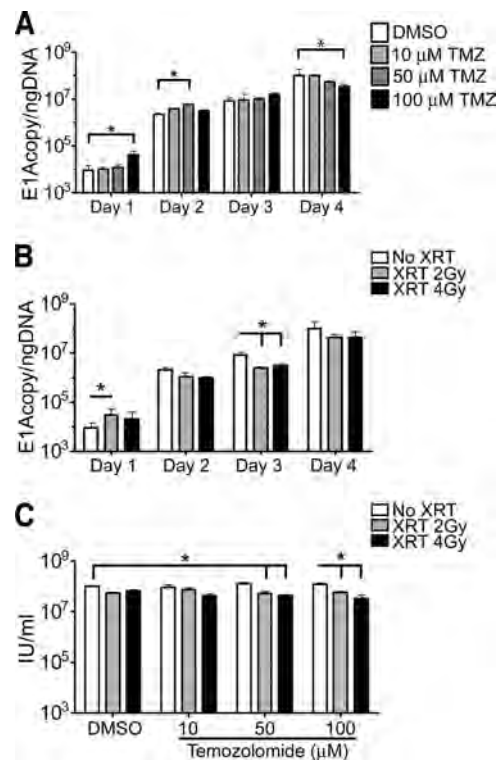


Figure 2. Evaluation of CRAd-Survivin-pk7 (CRAd-S-pk7) replication in neural stem cells (NSCs) treated with XRT-TMZ. Viral replication of CRAd-S-pk7 was measured by quantitative real-time polymerase chain reaction and presented as a number of viral E1A copies per nanogram of DNA from infected NSCs. (A, B): Viral replication was evaluated daily up to 96 hours after treatment with 0, 10, 50, or 100 μM TMZ (A) and 0, 2, or 4 Gy of XRT (B). (C): CRAd-S-pk7 viral titer levels 96 hours after XRT-TMZ treatment of infected NSCs. Treatment with both XRT and TMZ slightly reduced viral titer levels at high doses of TMZ, but no change was observed when treated with TMZ concentrations closer to physiologically relevant levels. *, $p < .05$. Abbreviations: DMSO, dimethyl sulfoxide; IU, infectious units; TMZ, temozolomide; XRT, radiation therapy.

we assessed viral progeny titers 96 hours after infection and noted that high-dose TMZ (50–100 μM) and radiation reduced production of infectious progeny in NSCs from $1.03 \times 10^8 \pm 2.2 \times 10^6$ IU/ml in untreated NSCs to $5.1 \times 10^7 \pm 9.4 \times 10^6$ IU/ml in NSCs treated with 2 Gy XRT and 50 μM TMZ (*, $p < .05$) (Fig. 2C). At the same time, NSCs treated with TMZ concentrations more closely related to those found to accumulate in the cerebral spinal fluid of patients ($\sim 5 \mu\text{M}$) [24, 26], and 2 Gy radiation had no significant effect on adenoviral progeny titers (Fig. 2C). Based on these data, we conclude that conventional therapy caused minimal interference with the ability of HB1.F3-CD cells to support therapeutic virus replication but did not increase CRAd-S-pk7 titers.

Loaded NSCs in Addition to Conventional Therapy Increase Glioma Cell Cytotoxicity In Vitro

We have previously shown that loaded NSCs can deliver the viral payload to glioma cells that are grown continuously under in vitro conditions [12]. Because long-term passage in vitro can alter glioma cell phenotype and molecular profile, we tested the sensitivity of the patient-derived glioma line GBM43 toward our adenovirus-loaded NSCs. GBM43 cells are passaged in mouse flanks and used for experiments without any in vitro passaging to

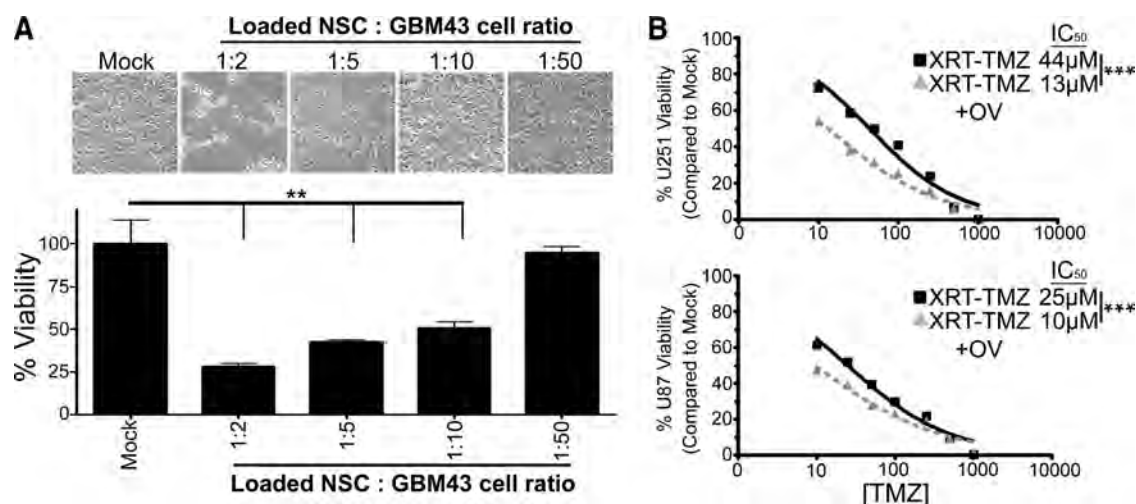


Figure 3. Antitumor effects of CRAd-Survivin-pk7 (CRAd-S-pk7)-loaded NSCs and their combination with XRT-TMZ against glioma cell lines in vitro. **(A):** Cytotoxicity of patient-derived GBM43 tumor cells 96 hours after coculture with CRAd-S-pk7-loaded NSCs at the NSC to GBM43 cell ratios of 1:0, 1:2, 1:5, 1:10, or 1:50. Top: Representative light microscope pictures of GBM43 viability. Bottom: Mean luciferase intensity values represented as the percentages of viable glioma cells compared with control. **(B):** U251 and U87 glioma cell viability measured by 3-(4,5-dimethylthiazol-2-yl)-2,5-diphenyltetrazolium bromide at 96 hours after treatment. The addition of CRAd-S-pk7 (50 infectious units) to conventional XRT-TMZ therapy reduced the percentage of glioma cell viability in both tested cell lines. The IC₅₀ values of TMZ for U251 and U87 cells when treated with XRT-TMZ decreased by 31 and 15 μM, respectively, when OV was added. **, $p < .01$; ***, $p < .001$. Abbreviations: NSC, neural stem cell; OV, oncolytic virus; TMZ, temozolomide; XRT, radiation therapy.

retain their original glioma characteristics [29, 30]. First, we tested whether loaded NSCs can induce toxicity to GBM43 when cocultured at different glioma to NSC ratios and found that adenovirus-loaded NSCs can induce significant toxicity up to a ratio of 1 NSC per 10 glioma cells at 96 hours after treatment (**, $p < .01$) (Fig. 3A).

Next, we tested whether CRAd-S-pk7 could enhance the therapeutic efficacy of conventional XRT-TMZ. U251 or U87 glioma cells were treated with conventional therapy consisting of 2 Gy XRT and varying concentrations of TMZ (0–1 × 10³ μM) or conventional treatment plus 50 IU of CRAd-S-pk7, and cell viability was measured by MTT at 96 hours. In both cell lines, combination therapy was more cytotoxic to glioma cells compared with conventional XRT-TMZ alone. The IC₅₀ values for TMZ decreased from 44 and 25 μM without oncolytic adenovirus infection to 13 and 10 μM when oncolytic virotherapy was added to the treatment of U251 and U87 glioma cells, respectively (***, $p < .001$) (Fig. 3B).

Oncolytic Adenovirus-Loaded NSCs Extend Survival of Glioma-Bearing Animals Treated With Conventional Chemo-Radiotherapy

In order to evaluate the therapeutic efficacy of OV-loaded NSCs (NSC-OV) in combination with XRT-TMZ therapy as compared with XRT-TMZ therapy alone, we first established a suboptimal treatment protocol for XRT-TMZ in vivo. This would allow us to assess whether our loaded NSCs could work jointly with conventional XRT-TMZ to increase the survival of animals bearing orthotopic human glioma xenografts. To test the combination therapy, we established a tumor model as described in Materials and Methods. The intracranial implantation of 3.5 × 10⁵ GBM43 cells results in an established tumor burden by day 1 of treatment (5 days after injection) as demonstrated by bioluminescence imaging and histological sections of mouse brains (supplemental online Fig. 2). We found that when mice bearing GBM43 were administered TMZ intraperitoneally at a dose of 30 mg/kg, the

majority of animals (four out of five) survived long term (>75 days), whereas, at the doses of 5 and 10 mg/kg, animals succumbed to the disease despite a significant increase in their survival when compared with mock-treated animals (***, $p < .001$) (Fig. 4A). We next looked at survival of mice receiving both XRT and TMZ simultaneously.

As shown in Figure 4B, 10 Gy fractionated radiotherapy (2 Gy per day for 5 days) alone prolonged median animal survival by 50% (16–24 days) when compared with mock-treated animals (**, $p < .01$). The addition of 2.5 mg/kg of TMZ proved no better than radiation alone, whereas 5 mg/kg of TMZ in combination with XRT increased animal survival by 7 days (from 24 to 31 days) when compared with XRT-treated animals (**, $p < .01$). When higher doses of TMZ (10 and 30 mg/kg) were administered in combination with XRT, most mice lived long term. Based on these results, we selected the suboptimal treatment regimen of 5 mg/kg of TMZ and 10 Gy of fractionated radiotherapy (2 Gy per day for 5 days) to test whether our CRAd-S-pk7-loaded NSCs added an additional survival benefit in an animal model of glioma.

Finally, to test the in vivo efficacy of the multimodality anti-glioma therapy, we first established intracranial GBM43 xenografts in nude mice. Five days after establishing intracranial glioma xenografts, the animals were injected with CRAd-S-pk7-loaded NSCs at two different doses: 5 × 10⁵ or 3 × 10⁶ (the maximum number of NSCs that could fit in a 2.5-μl injection volume) adenovirus-loaded NSCs. The next day, the animals began the previously established 5-day regimen of XRT-TMZ. As shown in Figure 4C, the intratumoral injection of 5 × 10⁵ loaded NSCs in combination with XRT-TMZ increased median survival by 29% over mice treated with XRT-TMZ alone. Furthermore, we observed a dose-dependent increase in the median survival time. When the number of OV-loaded NSCs was increased from 5 × 10⁵ to 3 × 10⁶, the median survival was increased by an additional 13% (5 × 10⁵ NSC-OV+XRT-TMZ-treated group = 31 days median survival; 3 × 10⁶ NSC-OV+XRT-TMZ-treated

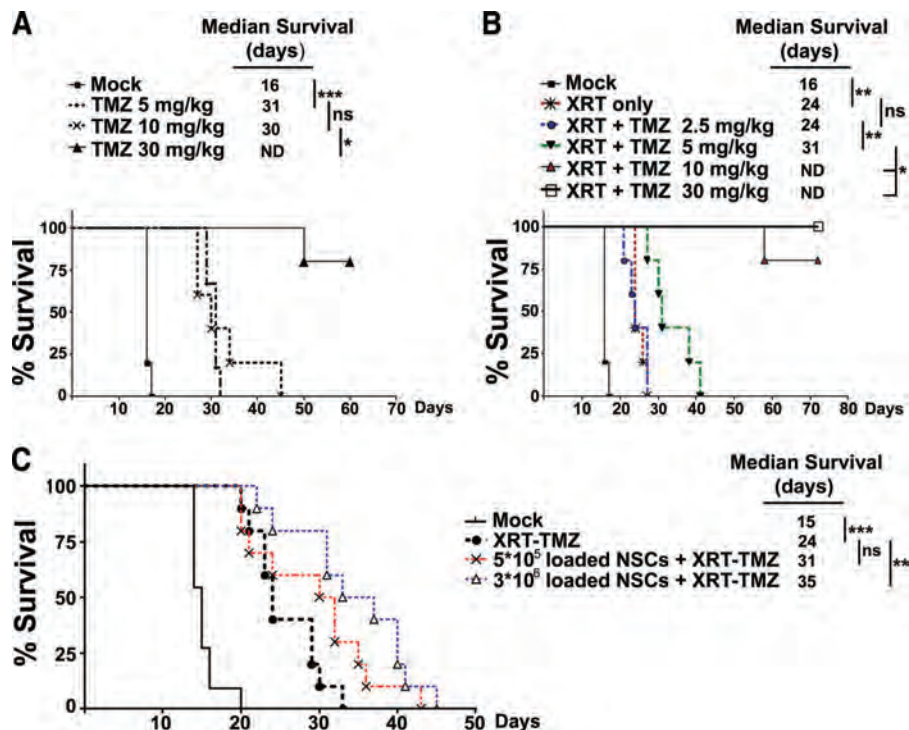


Figure 4. In vivo efficacy of CRAAd-Survivin-pk7 (CRAAd-S-pk7)-loaded NSCs and XRT-TMZ treatment against human-derived glioma xenografts. Intracranial GBM43 (3.5×10^5 cells per animal) was established, and the animals were treated for 5 consecutive days beginning on day 6 after tumor cell implantation. **(A):** Survival of animals treated with escalating doses of intraperitoneally administered TMZ (0, 5, 10, or 30 mg/kg). **(B):** Survival of animals treated with XRT (2 Gy) or a combination of XRT (2 Gy) and TMZ (2.5, 5, 10, or 30 mg/kg). **(C):** Survival of animals treated with the optimized dose of 2 Gy XRT and 5 mg/kg TMZ in addition to 5×10^5 or 3×10^6 loaded NSCs to XRT-TMZ treatment increased the median survival of glioma-bearing mice by 7 and 11 days, respectively. *, $p < .05$; **, $p < .01$; ***, $p < .001$. Abbreviations: ND, not determined; ns, no significance; NSC, neural stem cell; TMZ, temozolomide; XRT, radiation therapy.

group = 35 days median survival). Compared with XRT-TMZ treatment alone, the addition of 3×10^6 NSC-OV significantly increased the median survival by approximately 46% (XRT-TMZ-treated group = 24 days median survival; 3×10^6 NSC-OV+XRT-TMZ-treated group = 35-day median survival) (**, $p < .01$) (Fig. 4C).

Administration of Loaded NSCs Prior to Chemo-Radiotherapy Demonstrates the Greatest Survival Benefit

In the clinical setting there are two possible schedules when loaded NSCs could be realistically administered to patients: (a) before XRT-TMZ therapy and into the resection cavity during the time of surgery or (b) after XRT-TMZ therapy via an alternative clinical delivery approach if protocol specified. Depending on the mechanism of interaction, the relative timing and order of the treatment regimen could have a differential outcome on treatment efficacy, and therefore it is an important clinical consideration [31]. To determine which would provide the greatest benefit, we mimicked these scenarios both in vitro and in our animal model.

First, we tested both treatment approaches and measured cell toxicity in both U251 and U87 glioma cell lines. As shown in Figure 5A, glioma toxicity was dependent on the timing of OV administration. Both U87 and U251 cells showed greater toxicity at 96 hours when treated with oncolytic adenovirus (50 IU) 24 hours prior to treatment with TMZ (respective IC_{50} for each cell line) and 2 Gy XRT (*, $p < .05$; **, $p < .01$, respectively). Likewise, the patient-derived GBM39 cell line demonstrated more robust toxicity when treated with oncolytic adenovirus 24 hours prior to

XRT-TMZ (Rx) (***, $p < .001$). Furthermore, at 48 hours after treatment, GBM43 cells that were treated with CRAAd-S-pk7 virus 24 hours before XRT-TMZ resulted in a higher percentage of cells that stained positive for the active form of the caspase-3 protein (XRT-TMZ then OV = $8.7 \pm 0.4\%$ vs. OV then XRT-TMZ = $13.99 \pm 0.8\%$) (**, $p < .01$) (Fig. 5B). Together, this indicates that upfront treatment with OV induces higher levels of cellular apoptosis and cytotoxicity as compared with the alternative treatment approach.

We next considered a preclinical scheduling protocol to test whether the relative timing of loaded NSC administration had an effect on animal survival. To test this, we established GBM43 glioma xenografts in nude mice 5 days prior to the beginning of treatment. The mice were split into two treatment groups, and all mice received 5×10^5 loaded NSCs and 5 days of treatment with 5 mg/kg of TMZ and 2 Gy of XRT. To test timing as a variable for therapeutic outcome, we applied the following treatment schedules: (a) intratumoral (IT) injection of CRAAd-loaded NSCs followed by a full cycle of conventional therapy starting 24 hours later or (b) a full cycle of conventional therapy followed by an IT injection of CRAAd-loaded NSCs following its completion. What we observed in the animal model was consistent with the in vitro findings. As shown in Figure 6A, when animals received loaded NSCs before XRT-TMZ, their median survival was 9 days longer compared with the animals that received the reverse treatment schedule (*, $p < .05$). Furthermore, 33% of mice who received loaded NSCs before TMZ-XRT compared with 9% of mice who received the opposite treatment regimen lived long term (>70 days). In addition, the level of apoptosis in the mouse brain tumors corresponded to the increased survival

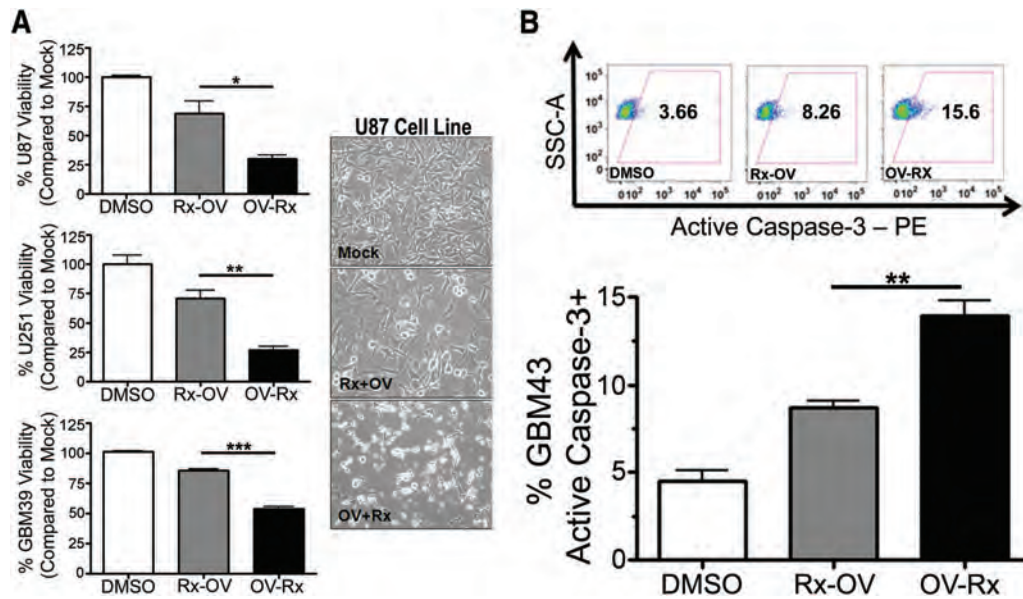


Figure 5. Optimization of combination therapy in vitro. **(A):** Cytotoxicity of U251 and U87 glioma cell lines and GBM39 patient-derived cell line treated with Rx-OV or OV-Rx. Left: The percentage of viability of glioma cells measured by 3-(4,5-dimethylthiazol-2-yl)-2,5-diphenyltetrazolium bromide 96 hours after treatment. Right: Representative light microscope pictures of U87 glioma cell viability (magnification, $\times 10$). **(B):** Percentage of apoptotic GBM43 cells at 48 hours after treatment with Rx-OV or OV-Rx treatment protocols as measured by the expression of active caspase-3-positive tumor cells by FACS (bottom). Top: Representative FACS plots. *, $p < .05$; **, $p < .01$; ***, $p < .001$. Abbreviations: DMSO, dimethyl sulfoxide; OV-Rx, ionizing radiation-temozolamide therapy 24 hours after oncolytic virus; PE, phycoerythrin; Rx-OV, oncolytic virus 24 hours after ionizing radiation-temozolamide therapy.

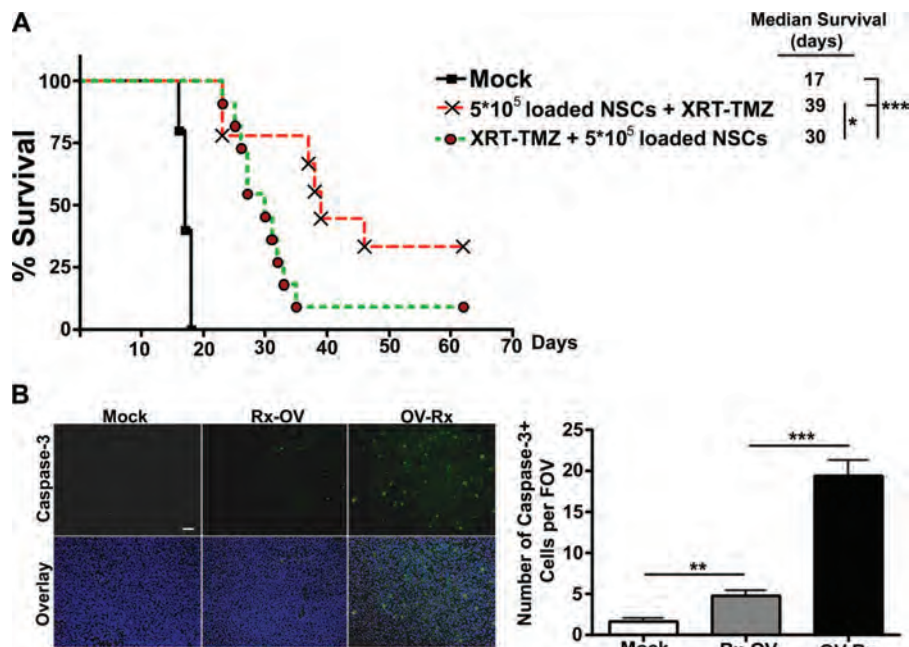


Figure 6. Scheduling of CRAd-Survivin-pk7 (CRAd-S-pk7)-loaded NSC administration in vivo. **(A):** Survival of animals treated with both therapeutic scheduling protocols. Intracranial GBM43 (3.5×10^5 cells per animal) was established, and the animals received an intratumoral (IT) injection of loaded NSCs (5×10^5) on day 5 followed by 5 consecutive days of XRT-TMZ (2 Gy and 5 mg/kg) therapy beginning on day 6 or alternatively XRT-TMZ therapy starting on day 6 for 5 consecutive days followed by an IT injection of loaded NSCs on day 12. A 9-day preferential median survival was observed in mice that received upfront NSC-based oncolytic therapy. **(B):** Fluorescent microscopy of mouse brain tissue bearing GBM43 xenografts (left). Top: Anti-cleaved caspase-3 (green). Bottom: Overlay; anti-cleaved caspase-3 (green) and anti-4',6-diamidino-2-phenylindole (blue). Magnification, $\times 20$. Scale bar = 50 μm . For each treatment group, five images were taken using the $\times 20$ objective, and the number of positive cells was quantified per field of view (right). *, $p < .05$; **, $p < .01$; ***, $p < .001$. Abbreviations: FOV, field of view; NSC, neural stem cell; OV-Rx, XRT-TMZ therapy 24 hours after oncolytic virus-loaded NSCs; Rx-OV, oncolytic virus-loaded NSCs 24 hours after XRT-TMZ therapy; TMZ, temozolamide; XRT, radiation therapy.

observed in mice treated with loaded NSCs prior to receiving XRT-TMZ. Immunohistopathological examination of the mouse brains from the two treatment groups revealed a significantly higher number of caspase-3-positive cells in the brain tumors of mice that received treatment with loaded NSCs 24 hours before treatment with standard therapy (Rx). The number of caspase-3-positive cells was counted per $\times 20$ objective field of view (FOV), and brain tumors treated with upfront loaded NSCs showed 19.40 ± 1.860 caspase-3-positive cells per FOV as compared with 4.800 ± 0.5831 caspase-3-positive cells per FOV in the brain tumors treated with the alternative treatment schedule (***, $p < .001$) (Fig. 6B). Based on these observations, we conclude that OV-loaded NSCs should be administered prior to conventional therapy.

CRAd-S-pk7 Radiosensitizes Glioma Cells by Inhibiting Radiation-Induced DNA Damage Responses

To elucidate the molecular mechanism responsible for the preferential survival observed in animals receiving loaded NSCs prior to conventional glioma therapy, we considered two possible explanations: (a) therapy is enhanced through an increase in oncolysis caused by a chemotherapy- and/or radiation-mediated increase in viral replication rates [32], or conversely, (b) OV induces a molecular change in tumor cells that leads to an improved response to chemo- or radiotherapy [33, 34]. Currently, the interaction between oncolytic adenovirus and conventional therapies for glioma remains unclear [35, 36]. Based on previously published data, in addition to evidence from our preliminary results that showed no significant increase in viral titers upon exposure to XRT-TMZ (Fig. 2C), we selected to investigate how CRAd-S-pk7 affects the DNA repair machinery of glioma cells. It has been shown that adenovirus oncoproteins, such as the E1B 55-kDa gene product, can inactivate the Mre11-Rad50-NBS1 (MRN) DNA repair complex in infected cells and suppress the hosts' DNA damage responses during viral DNA replication [33]. Based on this, we hypothesized that OV infection prior to conventional treatment can sensitize the infected glioma cells to radiotherapy.

To test this, we measured MRN complex protein levels by Western blot over time after infection with adenoviruses CRAd-S-pk7 and ONYX-015. As shown in Figure 7A, the levels of Rad50 and Mre11 protein gradually decreased over time after CRAd-S-pk7 infection in both U87 and U251 glioma cell lines. At 36 and 48 hours after infection, when the levels of Rad50 and Mre11 protein were at their lowest, the expression of MRN complex proteins remained unchanged in both U87 and U251 glioma cells infected with the E1B attenuated ONYX-015 adenovirus.

Furthermore, to investigate whether the observed decrease in MRN proteins after CRAd-S-pk7 infection could abrogate the DNA repair process in glioma cells in response to ionizing radiation, we measured the cells' ability to resolve γ H2AX foci, a sensitive indicator of DNA double-stranded breaks (DSBs), over time. GBM43 cells were treated with OV either 24 hours prior to or after XRT treatment and collected 24, 48, and 72 hours relative to the time when cells received irradiation. Immunofluorescent staining for γ H2AX foci revealed that at 72 hours, there were a greater number of γ H2AX foci in cells treated with OV before XRT compared with cells treated with XRT before OV or XRT alone (number of γ H2AX foci per cell: red arrows, 0–50 foci; yellow arrows, 51–100 foci; blue arrows, 101–200 foci; and orange arrows, >200 foci) (Fig. 7B, 7C). To quantify the rate of γ H2AX foci resolution over time, the number of foci per cell at

each consecutive time point was counted, and the effect over time was analyzed by ordinal logistic regression. Figure 7C reveals, in glioma cells that were irradiated 24 hours prior to receiving OV, a decreasing number of γ H2AX foci over time as the DNA DSBs were repaired (negative time effect; coefficient: -0.024 ± 0.01 ; $p = .020$). Furthermore, glioma cells that were treated with OV 24 hours before irradiation had static γ H2AX foci levels over time (no significant time effect; coefficient: 0.009 ± 0.01 ; $p = .386$). These results indicate that infection with CRAd-S-pk7 may increase the sensitivity of glioma cells to XRT treatment by compromising the cells' ability to repair DNA damage induced by ionizing radiation.

DISCUSSION

The investigation and development of superior treatment approaches for highly invasive and therapy-resistant glioblastoma are necessary. Over the past few years, our laboratory has developed the HB1.F3-CD NSC line into a cell carrier for specific delivery of the glioma tropic OV CRAd-S-pk7 in the preclinical setting [12]. At this stage we are currently conducting the necessary preclinical studies required to file for an IND application for the evaluation of NSC-based anti-glioma virotherapy in patients with newly diagnosed or recurrent malignant glioma.

Translating novel therapies from the laboratory to clinical trials is a complex path with many challenges [37]. Every day, promising gene therapy translational research is being conducted, but the outcomes of many phase III clinical trials fail to meet expectations. "Preclinical robustness" is the term coined to refer to how well preclinical studies are designed to accurately predict the efficacy of novel treatments in human patients. It is thought that in order to improve the success rate of novel therapies in clinical trials, preclinical studies need to become more robust. In order to increase the robustness of preclinical data, a novel therapy should be evaluated in a model that is most representative of the human disease and tested in conjunction with the standard of care treatment [38]. Although a challenging task, we feel that our studies and preclinical animal model meet several standards of preclinical robustness and therefore stringently support the application of OV-loaded NSCs for treatment of glioblastoma.

We first tested the function of our NSC carrier in the presence of conventional GBM therapies. A major advantage of a carrier cell-based system to deliver OV is the capacity of stem cells to transport therapeutics to their intended targets located at a distance from the original tumor site. It is critical that HB1.F3-CD cells retain their migratory capacity under an environment influenced by XRT-TMZ. Many signaling molecules have been implicated in the regulation of stem cell migration including CXCR4, CD44, VEGFR2, and uPAR [39]. Even though the CXCR4 and CD44 transcript levels were decreased in HB1.F3-CD cells upon XRT-TMZ exposure *in vitro*, we did not observe any alteration in the tumor-tropic migratory capacity of NSCs (Fig. 1). Although the mechanism is not yet proven, a wealth of convincing data exist showing that vascular endothelial growth factor (VEGF) is copiously expressed in glioma cells and is a strong chemoattractant mediating NSC migration [13, 40–42]. As shown in Figure 1B at 24 hours after XRT-TMZ therapy, NSCs retain their level of VEGFR2 gene expression compared with untreated cells. Taken together, conventional radio- and chemotherapy did not alter the VEGFR2 mRNA expression of NSCs or their migratory

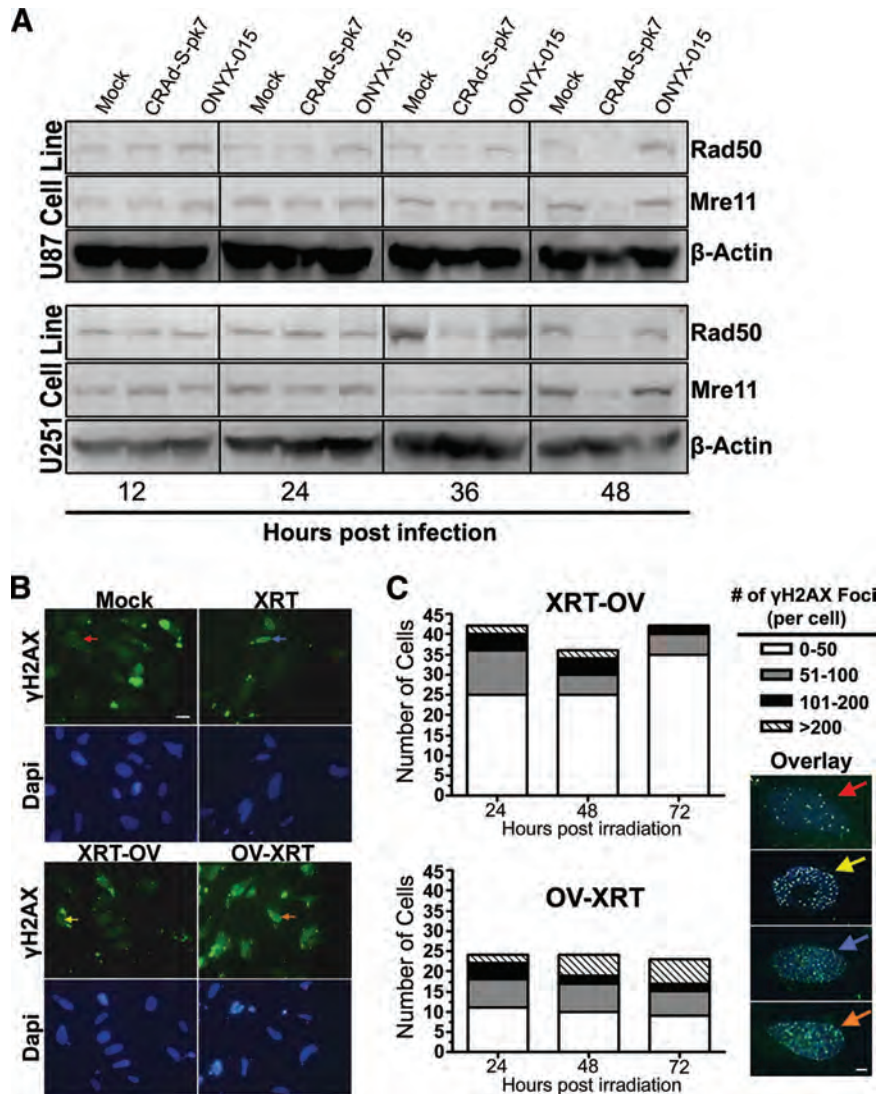


Figure 7. Radiosensitizing effect of CRAd-Survivin-pk7 (CRAd-S-pk7) infection on glioma. **(A):** Protein expression of the Mre11-Rad50-NBS1 complex proteins Rad50 (153 kDa) and Mre11 (81 kDa) at 12, 24, 36, and 48 hours after infection with 50 infectious units of CRAd-S-pk7 or ONYX-015. Western blots show that Rad50 and Mre11 protein expression are reduced at both 36 and 48 hours after infection with CRAd-S-pk7 but not ONYX-015. **(B):** Immunofluorescent staining of radiation induced γ H2AX foci under a confocal laser microscope. Top: Anti- γ H2AX (green); bottom: Dapi (blue). Magnification, $\times 63$. Scale bar = 20 μ m. **(C):** Quantification of γ H2AX foci resolution over 72 hours after XRT treatment. The number of γ H2AX foci per cell was counted and grouped according to the following range of foci per cell: 0–50 (red arrows), 51–100 (yellow arrows), 101–200 (blue arrows), and >200 (orange arrows). Left: Time effect was determined by ordinal logistic regression analysis. The number of γ H2AX foci was significantly resolved over time in XRT-OV-treated cells ($p = .020$), whereas there was no significant change in the number of foci over time in OV-XRT-treated cells ($p = .386$). Right: Representative overlay images of each range of foci per cell (anti- γ H2AX, green, and anti-DAPI, blue). Magnification, $\times 63$. Scale bar = 20 μ m. Abbreviations: Dapi, 4',6'-diamidino-2-phenylindole; OV-XRT, radiation therapy 24 hours after oncolytic virus; XRT-OV, oncolytic virus 24 hours after radiation therapy.

capacity, and therefore VEGF-VEGFR2 receptor signaling may be critical for maintaining the tumor pathotropism of HB1.F3-CD cells.

Another benefit of stem cell-based oncolytic virotherapy is the ability of OV-loaded stem cells to serve as in situ factories for viral replication. For this approach to work in conjunction with the standard of care for GBM, NSCs must retain their ability to support therapeutic virus replication. Despite our results that show a slightly diminished viral titer when NSCs are treated with radiation and high-dose chemotherapy on day 4, at lower doses of TMZ the viral titer was unaffected and remained consistent with the titer produced by untreated NSC carriers. Interestingly, although we did not see increased viral replication, we did ob-

serve an increased cytotoxic effect in both U251 and U87 glioma cell lines when cells were treated with OV in addition to XRT-TMZ (Fig. 3B), which we later attributed to the possible radiosensitizing effect of OV. To test the efficacy of CRAd-loaded NSCs in combination with conventional therapy in vivo, we established a preclinical model. In developing our model we considered factors that would influence the preclinical robustness of our experiments and addressed the shortcomings of previous animal models. Treating a tumor in its natural environment can significantly influence therapeutic outcome. Many previous studies evaluating the combination of OV and conventional therapy have been limited to subcutaneous tumor models [31] or intracranial models established from cell lines passaged in vitro. Therefore, we

chosed to establish intracranial orthotopic xenografts that were derived from an explanted patient GBM and serially passaged *in vivo*. Furthermore, because GBM patients receive surgery, followed by radiotherapy and temozolomide, it is crucial that novel therapies retain their utility when used with this treatment approach. To incorporate this aspect of the clinical scenario into our preclinical model, we tested the efficacy of concomitant TMZ and fractionated XRT [27] for 5 consecutive days in combination with stem cell-based oncolytic virotherapy (Fig. 4C). We believe that this model may capture some of the complexities of treating a human GBM in the clinic and contribute to the preclinical robustness of our results. Additionally, the extent of the disease burden during the time of administration may dictate the treatment effectiveness and therefore should be considered as a variable that may impact outcome. As we show in supplemental online Figure 2, the disease burden is established prior to treatment on day 5 after implantation. Moreover, in the clinical setting, we propose to administer CRAd-loaded NSCs after tumor resection and before the patient receives XRT and TMZ. During this time, depending on the extent of resection, approximately 95% of the original tumor volume has been removed [43]. In this case, the therapy is intended to treat the minimal volume of residual disease. Thus, because of the careful consideration while developing the xenograft model used in this study, we consciously attempted to mimic the clinical scenario with respect to disease burden at the proposed time of NSC-based anti-glioma oncolytic virus administration.

Finally, the timing of loaded NSC administration is an additional clinical variable that we explored because the relative timing of treatment could be important both logistically and therapeutically. We considered that loaded NSCs could be administered to patients before receiving the standard of care or afterward [38]. We concluded that loaded NSCs delivered up-front to conventional therapy may be the optimal time for their administration (Figs. 5, 6) in order to take advantage of their potential radiosensitizing effects. It is established that ionizing radiation produces a wide variety of lesions in the host DNA, including single- and DSBs, base damage, and cross-linking of DNA-DNA and DNA-protein [44]. DSBs play an important role in radiation-induced cell death and are considered to be a critical factor for the therapeutic efficacy of anti-cancer radiotherapy. Upon detection of DNA damage, cells activate the DNA repair pathway by initiating cell cycle arrest and inducing expression of various genes associated with DNA repair mechanisms. MRN is one protein complex that can act as a DSB sensor by rapidly binding to damaged DNA and serving as the link between DNA repair and the cell cycle regulatory pathway [45]. It has been reported that adenovirus 5 can effectively inactivate the MRN complex in infected cells that would otherwise inhibit viral DNA replication and packaging [46]. The viral E1B 55-kDa protein, with cooperation from the E4orf6 viral protein, sequesters the MRN complex in infected cells and induces proteasome-dependent degradation [33]. Expression of these viral genes in human colorectal carcinoma and GBM cell lines inhibits DNA DSB repair and induces a radiosensitizing effect in infected cells [47].

Based on this, we speculate that the advantage of administering OV-loaded NSCs prior to radiotherapy is the sensitizing effect of CRAd-S-pk7 on glioma cells toward radiotherapy, which one may not observe if OV-loaded NSCs are administered after XRT treatment. As shown in Figure 7A, the degradation of MRN proteins is most pronounced at 36–48 hours after adenoviral infection *in vitro*, but it is yet to be determined whether delivery of loaded NSCs 24 hours before the start of conventional therapy is the adequate amount of time to achieve a maximal survival advantage *in vivo*. Furthermore, although we show that loaded NSCs are compatible with TMZ both *in vitro* and *in vivo*, a further investigation into possible mechanisms of interaction is warranted.

CONCLUSION

In summary, we have demonstrated that stem cell-based oncolytic therapy is well suited to be administered with chemo-radiotherapy. We have shown that the increased efficacy observed with combination therapy is dependent on the relative timing of administration and that NSCs loaded with CRAd-S-pk7 should be given prior to XRT-TMZ therapy. The potential radiosensitization induced by adenovirus infection may be a powerful tool for targeting therapeutically resistant tumor cells, a hallmark of GBM's malignancy. Furthermore, the use of carrier cells can distribute oncolytic viruses throughout the brain to target disseminated tumor burdens. The future of GBM therapy is dependent on novel therapies, and this investigation has set the foundation for the clinical protocol of stem cell-based oncolytic therapy and brought it one step closer to clinical trials.

ACKNOWLEDGMENTS

This work was supported by the National Institute of Neurological Disorders and Stroke Grants U01-NS069997 and R01-NS077388 and National Cancer Institute Grants R01-CA122930 and K99-CA160775. We thank Shirley Bond from the Integrated Microscopy Core Facility at the University of Chicago for her microscopy support. We are grateful to Dr. C. David James for providing the patient-derived GBM lines GBM43 and GBM39.

AUTHOR CONTRIBUTIONS

A.L.T. and B.T.: collection and assembly of data, data analysis and interpretation, manuscript writing; B.A., E.R., I.V.B., C.K.K., and Y.H.: collection and assembly of data; L.Z.: data analysis and interpretation; K.S.A.: provision of the HB1.F3.CD cell line; A.U.A.: conception and design, manuscript writing; M.S.L.: conception and design, financial support, final approval of manuscript.

DISCLOSURE OF POTENTIAL CONFLICTS OF INTEREST

K.S.A. has uncompensated employment with TheraBiologics, Inc., is a coinventor on a preliminary patent, and holds stock options in TheraBiologics, Inc.

REFERENCES

1 Xu DS, Yang C, Proescholdt M et al. Neuronatin in a subset of glioblastoma multi-

forme tumor progenitor cells is associated with increased cell proliferation and shorter patient survival. *PLoS One* 2012;7:e37811.

2 Tran B, Rosenthal MA. Survival comparison between glioblastoma multiforme and other incurable cancers. *J Clin Neurosci* 2010; 17:417–421.

- 3 Thumma SR, Elaimy AL, Daines N et al. Long-term survival after gamma knife radiosurgery in a case of recurrent glioblastoma multiforme: A case report and review of the literature. *Case Report Med* 2012;2012:545492.
- 4 Rahman R, Smith S, Rahman C et al. Anti-angiogenic therapy and mechanisms of tumor resistance in malignant glioma. *J Oncol* 2010;2010:251231.
- 5 Grossman SA, Ye X, Piantadosi S et al. Survival of patients with newly diagnosed glioblastoma treated with radiation and temozolomide in research studies in the United States. *Clin Cancer Res* 2010;16:2443–2449.
- 6 Liu C, Zong H. Developmental origins of brain tumors. *Curr Opin Neurobiol* 2012;22:844–849.
- 7 Bao S, Wu Q, McLendon RE et al. Glioma stem cells promote radioresistance by preferential activation of the DNA damage response. *Nature* 2006;444:756–760.
- 8 Beier D, Schulz JB, Beier CP. Chemoresistance of glioblastoma cancer stem cells: Much more complex than expected. *Mol Cancer* 2011;10:128.
- 9 Kim SU, de Vellis J. Stem cell-based cell therapy in neurological diseases: A review. *J Neurosci Res* 2009;87:2183–2200.
- 10 Aboody KS, Brown A, Rainov NG et al. Neural stem cells display extensive tropism for pathology in adult brain: Evidence from intracranial gliomas. *Proc Natl Acad Sci USA* 2000;97:12846–12851.
- 11 Ulasov IV, Zhu ZB, Tyler MA et al. Survival-driven and fiber-modified oncolytic adenovirus exhibits potent antitumor activity in established intracranial glioma. *Hum Gene Ther* 2007;18:589–602.
- 12 Thaci B, Ahmed AU, Ulasov IV et al. Pharmacokinetic study of neural stem cell-based cell carrier for oncolytic virotherapy: Targeted delivery of the therapeutic payload in an orthotopic brain tumor model. *Cancer Gene Ther* 2012;19:431–442.
- 13 Ahmed AU, Thaci B, Alexiades NG et al. Neural stem cell-based cell carriers enhance therapeutic efficacy of an oncolytic adenovirus in an orthotopic mouse model of human glioblastoma. *Mol Ther* 2011;19:1714–1726.
- 14 Chatrchyan S, Khachatryan V, Sirunyan AM et al. Search for supersymmetry in pp collisions at $\sqrt{s}=7$ TeV in events with two photons and missing transverse energy. *Phys Rev Lett* 2011;106:211802.
- 15 Ahmed AU, Ulasov IV, Mercer RW et al. Maintaining and loading neural stem cells for delivery of oncolytic adenovirus to brain tumors. *Methods Mol Biol* 2012;797:97–109.
- 16 Tyler MA, Ulasov IV, Sonabend AM et al. Neural stem cells target intracranial glioma to deliver an oncolytic adenovirus in vivo. *Gene Ther* 2009;16:262–278.
- 17 Kanai R, Rabkin SD, Yip S et al. Oncolytic virus-mediated manipulation of DNA damage responses: Synergy with chemotherapy in killing glioblastoma stem cells. *J Natl Cancer Inst* 2012;104:42–55.
- 18 Karapanagiotou EM, Roulstone V, Twigger K et al. Phase I/II trial of carboplatin and paclitaxel chemotherapy in combination with intravenous oncolytic reovirus in patients with advanced malignancies. *Clin Cancer Res* 2012;18:2080–2089.
- 19 Immonen A, Vapalahti M, Tyynela K et al. AdvHSV-tk gene therapy with intravenous ganciclovir improves survival in human malignant glioma: A randomised, controlled study. *Mol Ther* 2004;10:967–972.
- 20 Kim SU, Nagai A, Nakagawa E et al. Production and characterization of immortal human neural stem cell line with multipotent differentiation property. *Methods Mol Biol* 2008;438:103–121.
- 21 Kim SK, Kim SU, Park IH et al. Human neural stem cells target experimental intracranial medulloblastoma and deliver a therapeutic gene leading to tumor regression. *Clin Cancer Res* 2006;12:5550–5556.
- 22 Sonabend AM, Ulasov IV, Han Y et al. Biodistribution of an oncolytic adenovirus after intracranial injection in permissive animals: A comparative study of Syrian hamsters and cotton rats. *Cancer Gene Ther* 2009;16:362–372.
- 23 Beier D, Rohrl S, Pillai DR et al. Temozolomide preferentially depletes cancer stem cells in glioblastoma. *Cancer Res* 2008;68:5706–5715.
- 24 Rosso L, Brock CS, Gallo JM et al. A new model for prediction of drug distribution in tumor and normal tissues: Pharmacokinetics of temozolomide in glioma patients. *Cancer Res* 2009;69:120–127.
- 25 Brada M, Judson I, Beale P et al. Phase I dose-escalation and pharmacokinetic study of temozolomide (SCH 52365) for refractory or relapsing malignancies. *Br J Cancer* 1999;81:1022–1030.
- 26 Ostermann S, Csajka C, Budlin T et al. Plasma and cerebrospinal fluid population pharmacokinetics of temozolomide in malignant glioma patients. *Clin Cancer Res* 2004;10:3728–3736.
- 27 Stupp R, Mason WP, van den Bent MJ et al. Radiotherapy plus concomitant and adjuvant temozolomide for glioblastoma. *N Engl J Med* 2005;352:987–996.
- 28 Ahmed AU, Lesniak MS. Glioblastoma multiforme: Can neural stem cells deliver the therapeutic payload and fulfill the clinical promise? *Expert Rev Neurother* 2011;11:775–777.
- 29 Sarkaria JN, Carlson BL, Schroeder MA et al. Use of an orthotopic xenograft model for assessing the effect of epidermal growth factor receptor amplification on glioblastoma radiation response. *Clin Cancer Res* 2006;12:2264–2271.
- 30 Giannini C, Sarkaria JN, Saito A et al. Patient tumor EGFR and PDGFRA gene amplifications retained in an invasive intracranial xenograft model of glioblastoma multiforme. *Neuro Oncol* 2005;7:164–176.
- 31 Ottolino-Perry K, Diallo JS, Lichty BD et al. Intelligent design: Combination therapy with oncolytic viruses. *Mol Ther* 2010;18:251–263.
- 32 Kim SH, Wong RJ, Kooby DA et al. Combination of mutated herpes simplex virus type 1 (G207 virus) with radiation for the treatment of squamous cell carcinoma of the head and neck. *Eur J Cancer* 2005;41:313–322.
- 33 Stracker TH, Carson CT, Weitzman MD. Adenovirus oncoproteins inactivate the Mre11-Rad50-NBS1 DNA repair complex. *Nature* 2002;418:348–352.
- 34 Kuroda S, Fujiwara T, Shirakawa Y et al. Telomerase-dependent oncolytic adenovirus sensitizes human cancer cells to ionizing radiation via inhibition of DNA repair machinery. *Cancer Res* 2010;70:9339–9348.
- 35 Bieler A, Mantwill K, Holzmüller R et al. Impact of radiation therapy on the oncolytic adenovirus dl520: Implications on the treatment of glioblastoma. *Radiother Oncol* 2008;86:419–427.
- 36 Georger B, Grill J, Opolon P et al. Potentiation of radiation therapy by the oncolytic adenovirus dl1520 (ONYX-015) in human malignant glioma xenografts. *Br J Cancer* 2003;89:577–584.
- 37 Tobias A, Ahmed A, Moon KS et al. The art of gene therapy for glioma: A review of the challenging road to the bedside. *J Neurol Neurosurg Psychiatry* 2013;84:213–222.
- 38 Lowenstein PR, Castro MG. Uncertainty in the translation of preclinical experiments to clinical trials: Why do most phase III clinical trials fail? *Curr Gene Ther* 2009;9:368–374.
- 39 Zhao D, Najbauer J, Garcia E et al. Neural stem cell tropism to glioma: Critical role of tumor hypoxia. *Mol Cancer Res* 2008;6:1819–1829.
- 40 Heidenreich R, Machein M, Nicolaus A et al. Inhibition of solid tumor growth by gene transfer of VEGF receptor-1 mutants. *Int J Cancer* 2004;111:348–357.
- 41 Schmidt NO, Przylecki W, Yang W et al. Brain tumor tropism of transplanted human neural stem cells is induced by vascular endothelial growth factor. *Neoplasia* 2005;7:623–629.
- 42 Zhang H, Vutskits L, Pepper MS et al. VEGF is a chemoattractant for FGF-2-stimulated neural progenitors. *J Cell Biol* 2003;163:1375–1384.
- 43 Bloch O, Han SJ, Cha S et al. Impact of extent of resection for recurrent glioblastoma on overall survival: Clinical article. *J Neurosurg* 2012;117:1032–1038.
- 44 Helleday T, Petermann E, Lundin C et al. DNA repair pathways as targets for cancer therapy. *Nat Rev Cancer* 2008;8:193–204.
- 45 Petrini JH. The mammalian Mre11-Rad50-nbs1 protein complex: Integration of functions in the cellular DNA-damage response. *Am J Hum Genet* 1999;64:1264–1269.
- 46 Karen KA, Hoey PJ, Young CS et al. Temporal regulation of the Mre11-Rad50-Nbs1 complex during adenovirus infection. *J Virol* 2009;83:4565–4573.
- 47 Hart LS, Yannone SM, Naczki C et al. The adenovirus E4orf6 protein inhibits DNA double strand break repair and radiosensitizes human tumor cells in an E1B–55K-independent manner. *J Biol Chem* 2005;280:1474–1481.



See www.StemCellsTM.com for supporting information available online.